

This is the preprint version of the contribution published as:

Zech, A., D'Angelo, C., Attinger, S., Fiori, A. (2018):

Revisitation of the dipole tracer test for heterogeneous porous formations

Adv. Water Resour. **115**, 198 – 206

The publisher's version is available at:

<http://dx.doi.org/10.1016/j.advwatres.2018.03.006>

Revisitation of the dipole tracer test for heterogeneous porous formations

Alraune Zech^{a,*}, Claudia D'Angelo^b, Sabine Attinger^{a,c}, Aldo Fiori^b

^a*Department of Computational Hydrosystems, Helmholtz Centre for Environmental Research - UFZ, Leipzig, Germany*

^b*Dipartimento di Ingegneria, Universita di Roma Tre, Rome, Italy*

^c*Institute for Geosciences, Friedrich Schiller University, Jena, Germany*

Abstract

In this paper, a new analytical solution for interpreting dipole tests in heterogeneous media is derived by associating the shape of the tracer breakthrough curve with the log-conductivity variance. It is presented how the solution can be used for interpretation of dipole field test in view of geostatistical aquifer characterization on three illustrative examples.

The analytical solution for the tracer breakthrough curve at the pumping well in a dipole tracer test is developed by considering a perfectly stratified formation. The analysis is carried out making use of the travel time of a generic solute particle, from the injection to the pumping well. Injection conditions are adapted to different possible field setting. Solutions are presented for resident and flux proportional injection mode as well as for an instantaneous pulse of solute and continuous solute injections.

The analytical form of the solution allows a detailed investigation on the impact of heterogeneity, the tracer input conditions and ergodicity conditions at the well. The impact of heterogeneity manifests in a significant spreading of solute particles that increases the natural tendency to spreading induced by the dipole setup. Furthermore, with increasing heterogeneity the number of layers needed to reach ergodic conditions become larger. Thus, dipole test in highly heterogeneous aquifers might take place under non-ergodic conditions giving that the log-conductivity variance is underestimated. The method is a promising geostatistical analyzing tool being the first analytical solution

*Corresponding Author

Email address: alraune.zech@ufz.de (Alraune Zech)

for dipole tracer test analysis taking heterogeneity of hydraulic conductivity into account.

Keywords:

- Analytical solution for breakthrough curve (BTC) of dipole tracer tests in heterogeneous media
- Interpretation of dipole field tests and estimation of aquifer heterogeneity (log-conductivity variance)
- Main features of dipole tests (strong preferential flow and persistent tail) are further strengthened by heterogeneity

1. Introduction

Groundwater is an important natural resource for drinking water supply. Hence, the investigation and predictive modeling of flow and transport in porous media are of broad relevance in particular for water quality aspects and methods for contaminated site treatment like remediation, risk assessment, and natural attenuation. Tracer tests are thereby the foremost used observation method for inferring hydrogeological, structural and transport parameters of the subsurface. Most important, the hydraulic conductivity K , which determines the velocity of groundwater flow, typically exhibits a large spatial heterogeneity with values varying over orders of magnitudes (Gelhar, 1993).

A bunch of different tracer test types exist which all have their merits but also limitations. Tracer test under ambient flow conditions are either limited to short travel distances, because groundwater flow is usually very slow, or the test operation suffers high costs due to a long test duration and the need for a large observation network. More efficient in time and size of observation network are tracer tests under forced flow conditions due to higher velocities and directed flow. However, the analysis of test types under well flow conditions are more complex due to the non-uniform flow field. Especially taking aquifer heterogeneity into account requires sophisticated analyzing methods.

In dipole tracer tests, also named two-well test or doublet tests, a tracer is introduced at a recharge well and the breakthrough curve (BTC) is measured at a pumping well. The pumped water can optionally be used for recharge in

25 a recirculation. The test setting has the advantage of circumventing the prob-
26 lem of removal of waste water and the need for an additional water source.
27 However, the complex flow pattern causes the interpretation of the transport
28 behavior to be more complicated. The dipole shape of the flow field gives
29 that the observed concentration at the pumping well to be a superposition
30 of tracer transport along different streamlines with different tracer arrival
31 times. The foremost aim in this work is to present an alternative inter-
32 pretation method for dipole tests in heterogeneous media. It will be given
33 a simple solution for interpretation of dipole test in view of geostatistical
34 aquifer characterization.

35 The first analytical analysis of dipole test was performed by Hoopes and
36 Harleman (1967). They presented a mathematical description of the flow
37 field, provided equations for streamlines and the travel time of a tracer par-
38 ticle along a streamline. They gave analytical expressions for the temporal
39 and spatial distribution of tracer in a homogeneous aquifer. By analyzing an
40 approximate solutions for the concentration in the presence of convection,
41 dispersion and diffusion, Hoopes and Harleman (1967) analyzed the impact
42 of these processes. They found that dispersion impacts only the very early
43 part of the BTC, afterwards the arrival of different streamlines is dominant.
44 For constant tracer injection, the BTC is almost insensitive to dispersion.

45 Shortly after, Grove and Beetem (1971) presented a method for analyzing
46 BTC of dipole tests in homogeneous aquifers in order to evaluate the porosity
47 and the longitudinal dispersivity. The method focuses on tests with pulse
48 tracer injection and recirculation being constructed as superposition of 1D
49 solutions for individual streamlines based on calculations of the streamline
50 length and particle travel time. The approach took the crucial assumption
51 that velocity is constant along flow lines. The work of Grove and Beetem
52 (1971) also included an illustrative example of an analysis of a dipole test in
53 the fractured carbonate aquifer near Carlsbad, New Mexico.

54 Gelhar (1982) derived a semi-analytical solution and provided type curves
55 for the BTC measured at the pumping well in a dipole flow system. The type
56 curves were numerically derived based on the theoretical work of Gelhar and
57 Collins (1971) about longitudinal dispersion along streamlines in nonuniform
58 flow. For the solution, transverse dispersion is assumed to be negligible. The
59 work of Gelhar (1982) included the analysis of a dipole test at the Hanford
60 Site for illustrating the method. Welty and Gelhar (1989) reanalyzed several
61 field tests using the method of Gelhar (1982) in order to estimate dispersivity.

62 The first approach to numerically interpret dipole tests was presented

63 by Huyakorn et al. (1986a). They developed a problem adapted simulation
64 software making use of a curvilinear FEM. The method was applied to the
65 dipole field test at the Chalk River site (Pickens and Grisak, 1981). More
66 recently, Bianchi et al. (2011) presented a numerical model to interpret the
67 dipole test at the MADE site with explicitly including aquifer heterogeneity.
68 The authors performed simulations with conditioned log-normal hydraulic
69 conductivity fields.

70 Several examples for dipole field tests in consolidated media can be found
71 in literature, mostly as illustrative examples along analytical method devel-
72 opment, e.g. in the previously mentioned papers of Grove and Beetem (1971);
73 Gelhar (1982); Welty and Gelhar (1989). Some early works on tracer tests re-
74 port large distance dipole tests. Examples are the test at the Savannah River
75 Plant (Webster et al., 1970) where wells are 538 m (1,765 feet) apart with a
76 duration of 2 years or the test at Amargosa (Claasen and Cordes, 1975) over a
77 distance of 122 m (400 feet). There are also several examples for tests in con-
78 solidated media, mostly over shorter ranges which a well distance maximally
79 a few tenths of meters, for instance Tucson, Arizona (Wilson, 1971); Chalk
80 River Site, Canada (Pickens and Grisak, 1981); Kesterson Aquifer, California
81 (Hyndman and Gorelick, 1996); Rocky Mountain Arsenal, Colorado (Thor-
82 bjarnarson and Mackay, 1997). Tests of particular interest within this work
83 are the dipole tests at MADE (Bianchi et al., 2011), Barstow (Robson, 1974),
84 and Mobile (Molz et al., 1986). They will act as illustrative examples for the
85 method developed herein and will be described in detail later.

86 Dipole tests in the presence of significant spatial heterogeneity of hy-
87 draulic conductivity have rarely been studied. Though, the actual streamline
88 structure of dipole tests is strongly impacted by aquifer heterogeneity. The
89 analysis of dipole test with an explicit representation of aquifer heterogene-
90 ity has been done only using numerical models, e.g. Bianchi et al. (2011).
91 Analytical models for dipole analysis including heterogeneity parameters are
92 not available. The methods of Hoopes and Harleman (1967); Grove and
93 Beetem (1971); Gelhar (1982); Welty and Gelhar (1989) are conceptualized
94 for homogeneous conductivity, taking the effect of aquifer heterogeneity only
95 implicitly into account by the lumped parameter of macrodispersivity.

96 In this paper, we present an alternative concept for dipole test analysis by
97 taking heterogeneity of hydraulic conductivity explicitly into account. A geo-
98 statistical approach is used due to the limited data availability in subsurface
99 hydrology in combination with high uncertainty in values. The character-
100 istics of hydraulic conductivity K are captured by the one-point statistical

101 parameters of mean conductivity K_G and the log-conductivity variance σ_Y^2 ,
102 with $Y = \ln K$ the log-conductivity. An analytical solution for the BTC at
103 the pumping well in a dipole tracer test is developed by considering a strat-
104 ified heterogeneous hydraulic conductivity structure, thus associating shape
105 of BTC with statistical properties of the conductivity field. The stochastic
106 framework and part of the analysis have some similarities with the model
107 presented by Pedretti and Fiori (2013) for convergent flow. The sensitivity
108 of dipole tests to spatial heterogeneity might be used to determine statistical
109 parameters, especially the log-conductivity variance σ_Y^2 offering an alterna-
110 tive test method for geostatistical aquifer analysis.

111 The plan of the paper is given as following: the mathematical framework
112 sets the background of the method providing the derivation of the analytical
113 solutions for different test configurations; it is followed by an illustration of
114 results and then a discussion on the impact of parameters and test condi-
115 tions on the BTC; the method is then used for conductivity characterization
116 on illustrative examples with a re-interpretation of three dipole field tests
117 with the newly developed method. The paper ends with a summary and
118 conclusions.

119 2. Mathematical framework

120 We consider a confined aquifer of thickness L ; the heterogeneous hydraulic
121 conductivity K field is modeled by considering the aquifer as a perfectly
122 stratified formation, i.e. made up from N layers of vertical thickness $2I$,
123 with I the vertical integral scale of hydraulic conductivity. Each layer is of
124 random and independent conductivity K_i ($i = 1, \dots, N$).

125 The justification of the stratified model is in the relative short distance
126 between pumping and injecting wells in dipole tests which is often found
127 in recent applications, of the order of the horizontal integral scale of K or
128 even less. The perfectly stratified formation has been often used in the
129 past for modeling flow and transport in heterogeneous porous formations,
130 often leading to useful analytical solutions (Mercado, 1967; Matheron and
131 De Marsily, 1980; Dagan, 1990).

132 A dipole is created by injecting and extracting a discharge Q in two fully
133 penetrating wells at relative distance $2a$. Adopting head boundary conditions
134 in the wells, the piezometric head does not depend on the vertical coordinate;
135 thus, the distribution of head is the same for all layers. A sketch of the
136 conceptual model is provided in Figure 1.

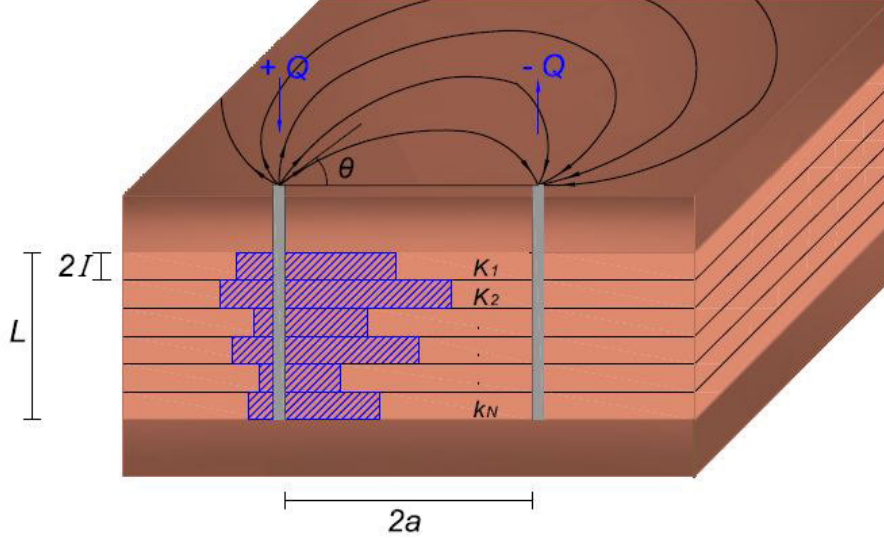


Figure 1: Illustration sketch of the conceptual model.

137 The discharge per unit thickness q_i for each layer i is equal to

$$q_i = \frac{K_i}{\bar{K}} q \quad (1)$$

138 with $\bar{K} = N^{-1} \sum_{i=1}^N K_i$ the arithmetic mean of K_i and $q = Q/L$ the
 139 aquifer discharge per unit depth.

140 At a given initial time, a pulse of solute of initial concentration C_0 and du-
 141 ration Δ is introduced in the injection well. The solute travels in the porous
 142 medium and it is collected downstream in the pumping well, resulting in a
 143 breakthrough curve (BTC) at the same well. The BTC, which corresponds
 144 to the temporal behavior of solute flux at the pumping well, depends on
 145 both the dipole setup (e.g. the distance $2a$, the discharge Q , the duration Δ
 146 etc) and the medium configuration, i.e. the vertical distribution of hydraulic
 147 conductivities K_i and their porosity, which in the following is assumed as
 148 constant in the entire domain.

149 Scope of the present analysis is to calculate the BTC in dependence on
 150 both the dipole setting and the aquifer configuration. The analysis is car-
 151 ried out by considering the travel time of a generic solute particle, from the

152 injection to the pumping well. It is well known, that the probability den-
 153 sity function (PDF) of such travel time is identical to the BTC of a solute
 154 instantaneous pulse. In the following we focus on advection only, which is
 155 the most significant source of spreading due to the non-uniform flow con-
 156 figuration. Local dispersion mechanisms like hydrodynamic dispersion or
 157 molecular diffusion are neglected.

158 The present solution is based on the analysis of Hoopes and Harleman
 159 (1967). They analyzed the travel time t of a particle, from the injection
 160 to the extraction well, pertaining to the generic streamline departing from
 161 the injection well at an angle θ with respect to the line joining the wells
 162 (see Figure 1). They derived an analytical solution for travel time in ho-
 163 mogeneous formations under the assumption that the aquifer is indefinite,
 164 homogeneous and isotropic and confined between two horizontal planes, in
 165 absence of natural flow. The flow and piezometric head were obtained from
 166 the superposition of the flow fields of a line source and a line sink, assuming
 167 negligible well radii. The flow fields are obtained by the solution of water
 168 continuity equations and Darcy's law. The travel time t was obtained by in-
 169 tegration of the flow field along the streamlines originating from the injection
 170 well. The resulting formula for the travel time in an arbitrary layer i is

$$t = \frac{4\pi na^2}{q_i \sin^2 \theta} (1 - \theta \cot \theta) \quad (-\pi \leq \theta \leq \pi) \quad (2)$$

171 with being n the constant porosity, q_i is the layer's unit discharge, θ is
 172 the angle and $2a$ is the distance between injection and pumping well.

173 Hereinafter we work with the dimensionless travel time τ , defined as

$$\tau = \frac{qt}{4\pi na^2} = g(\theta) \frac{\bar{K}}{K_i} \quad (3)$$

174 where

$$g(\theta) = \frac{1}{\sin^2 \theta} (1 - \theta \cot \theta) \quad (4)$$

175 The form of the dimensionless travel time result from the by definition
 176 $\tau = v_c t / s_c$ with $v_c = q/n$ being the characteristic velocity and $s_c = 4\pi a$ being
 177 a characteristic length scale. τ is symmetrical with respect to $\theta = 0$, and the
 178 half space $\theta = [0; \pi]$ can be safely considered in the analysis.

179 The travel time (3) is a random variable, that depends on the hydraulic
 180 conductivity K_i of each layer and the angle of attack θ , which is uniformly

181 distributed in the interval $[0; \pi]$. From (3) one can calculate the travel time
 182 distribution for the entire aquifer formation, considering the dependence of
 183 τ on the random variables K and θ , which distributions are $f_K(K)$ and
 184 $f_\theta = 1/\pi$, respectively. From basic statistics (see, e.g. Papoulis (1991)), the
 185 cumulative density function (CDF) P_τ of τ follows as

$$P_\tau(\tau) = \int \int_D f_K(K) f_\theta(\theta) dK d\theta = \frac{1}{\pi} \int_0^\pi \int_{g(\theta)\bar{K}/\tau}^\infty f_K(K) dK d\theta \quad (5)$$

186 where D is the region in the (θ, K) space such that $g(\theta)\bar{K}/K \leq \tau$.

187 Assuming ergodicity gives $\bar{K} = K_A$, with K_A being the arithmetic (en-
 188 semble) mean. The integration of (5) over K yields

$$P_\tau(\tau) = \frac{1}{\pi} \int_0^\pi \{1 - P_K(g(\theta)K_A/\tau)\} d\theta \quad (6)$$

189 with P_K being the CDF of K . From the above expression, the travel time
 190 PDF is calculated as

$$f_\tau^R(\tau) = \frac{1}{\pi} \frac{K_A}{\tau^2} \int_0^\pi g(\theta) f_K(g(\theta)K_A/\tau) d\theta \quad (\text{resident injection mode}) \quad (7)$$

191 If we assume a log-normal distribution for K , the above specializes as
 192 follows

$$f_\tau^R(\tau) = \frac{1}{\pi\tau\sqrt{2\pi\sigma_Y^2}} \int_0^\pi \exp\left[-\frac{(\sigma_Y^2/2 + \ln g(\theta) - \ln \tau)^2}{2\sigma_Y^2}\right] d\theta \quad (8)$$

193 Expression (7) is the PDF of the dimensionless travel time τ . In its cal-
 194 culation we have assumed that the mass of solute entering in each layer from
 195 the injection well is constant for all layers, i.e. the injection condition is
 196 of *resident concentration*. Instead, the typical injection condition in appli-
 197 cations is of *flux proportional*, i.e. the mass of solute entering each layer is
 198 proportional to the local velocity at the injection well, which is variable in the
 199 vertical and is proportional to the hydraulic conductivity K_i of each layer.
 200 The different injection conditions and their impact on the BTC is deeply
 201 discussed in Jankovic and Fiori (2010) for transport in mean uniform flow
 202 and in Pedretti and Fiori (2013) for transport in convergent flow.

203 The travel time PDF for flux proportional injection mode, along the above
 204 lines, can be calculated by weighting each solute particle by the layer conduc-
 205 tivity K_i . This way, the resulting travel time PDF is obtained by averaging
 206 the PDF (7) by the weight

$$\frac{K_i}{K_A} = \frac{g(\theta)}{\tau} \quad (9)$$

207 obtaining

$$f_{\tau}^F(\tau) = \frac{1}{\pi} \frac{K_A}{\tau^3} \int_0^{\pi} g^2(\theta) f_K(g(\theta) K_A/\tau) d\theta \quad (\text{flux-proportional injection mode}) \quad (10)$$

208 Assuming a log-normal distribution for K the latter becomes

$$f_{\tau}^F(\tau) = \frac{1}{\pi \tau^2 \sqrt{2\pi\sigma_Y^2}} \int_0^{\pi} g(\theta) \exp\left[-\frac{(\sigma_Y^2/2 + \ln g(\theta) - \ln \tau)^2}{2\sigma_Y^2}\right] d\theta \quad (11)$$

209 Summarizing, expression (10) represents the travel time PDF under flux
 210 proportional injection mode, that is the one to be used in applications.

211 The above solutions correspond to the BTC for an instantaneous pulse of
 212 solute. The extensions for continuous solute injections of initial concentration
 213 C_0 and duration Δ , which are typically employed in the tracer tests, are
 214 calculated by the convolution

$$C(\tau) = \int_0^{t^*} C_0(t') f_{\tau}(\tau - t') dt' \quad (12)$$

215 where

$$t^* = \begin{cases} \tau & \text{when } \tau \leq \delta \\ \delta & \text{when } \tau \geq \delta \end{cases} \quad \left(\delta = \frac{q\Delta}{4\pi na^2} \right) \quad (13)$$

216 In the simple but relevant case when C_0 is constant and K is log-normally
 217 distributed (i.e. when f_{τ} is equal to 11), (12) becomes

$$\frac{C(\tau)}{C_0} = \begin{cases} \Phi(\tau) & \text{when } \tau \leq \delta \\ \Phi(\tau) - \Phi(\tau - \delta) & \text{when } \tau > \delta \end{cases} \quad (14)$$

218 where

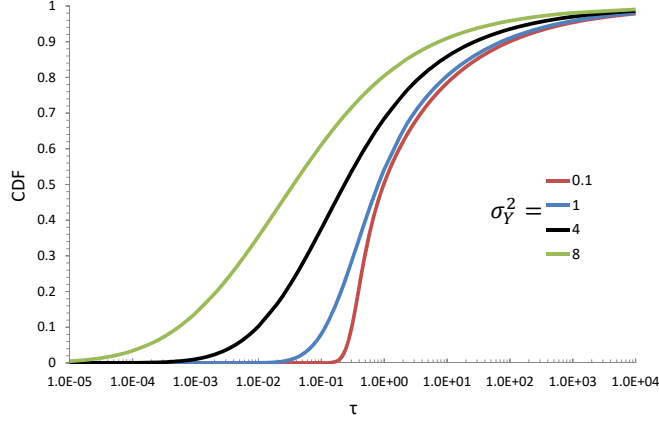


Figure 2: The travel time CDF P_τ^F as function of the dimensionless travel time $\tau = qt/(4\pi na^2)$ for a few values of the log-conductivity variance σ_Y^2 .

$$\Phi(\tau) = \frac{1}{2\pi} \int_0^\pi \left\{ 1 + \operatorname{erf} \left(\frac{\sigma_Y^2/2 - \ln g(\theta) + \ln(\tau)}{\sqrt{2\sigma_Y^2}} \right) \right\} d\theta \quad (15)$$

219 Formula (14) is the final result of the present analysis and provides the
 220 solute BTC for the dipole configuration examined here. The formula can be
 221 conveniently applied to the interpretation of dipole tests. We remind that
 222 the above solutions consider that the vertical distribution of conductivity
 223 is fully sampled, i.e. ergodicity is assumed; such condition is typically met
 224 when $L/I \gg 1$. The issue shall be further discussed in the next sections.

225 3. Illustration of results

226 In this section we illustrate the main results related to the proposed an-
 227 analytical solutions for the dipole tracer test. The PDF of the dimensionless

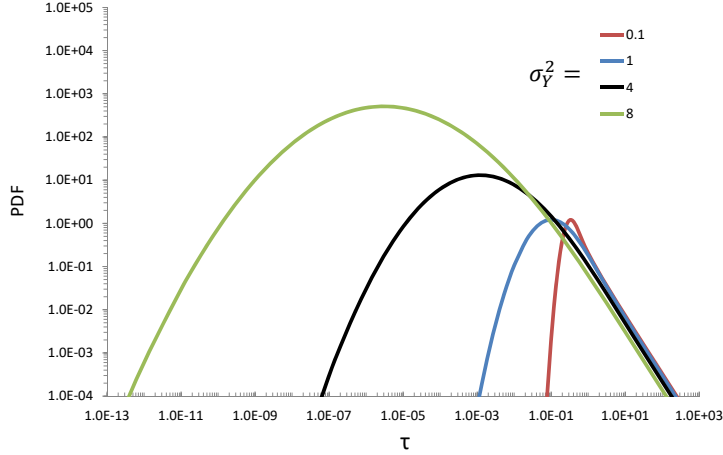


Figure 3: The travel time PDF f_{τ}^F as function of the dimensionless travel time $\tau = qt/(4\pi na^2)$ for a few values of the log-conductivity variance σ_Y^2 .

228 travel time $\tau = qt/(4\pi na^2)$ for the flux -proportional injection condition and
 229 a log-normal distribution of K is given by (11); the latter depends only on the
 230 log-conductivity variance σ_Y^2 , which represents the degree of heterogeneity of
 231 the aquifer system.

232 Figures 2 and 3 display the travel time PDF (P_{τ}^F) and CDF (f_{τ}^F) for a few
 233 values of σ_Y^2 , respectively. Starting from an almost homogeneous formation
 234 ($\sigma_Y^2 = 0.1$), it is seen that the distribution of τ is characterized by a rising
 235 limb, which is determined by the first "fast" arrivals of solute moving along
 236 the most connected paths between the injection and pumping wells (small
 237 angle θ). In turn, the tail of the distribution is typically long and persistent,
 238 being determined by the slow arrivals of solute particles that move along
 239 the longer and slower path lines (large θ). Thus, the dipole setup always
 240 determines a wide variety of paths in the medium, causing a similar variability
 241 of arrival times and hence dispersion; this is a well known feature which has
 242 already been described in past work (Hoopes and Harleman, 1967; Grove and

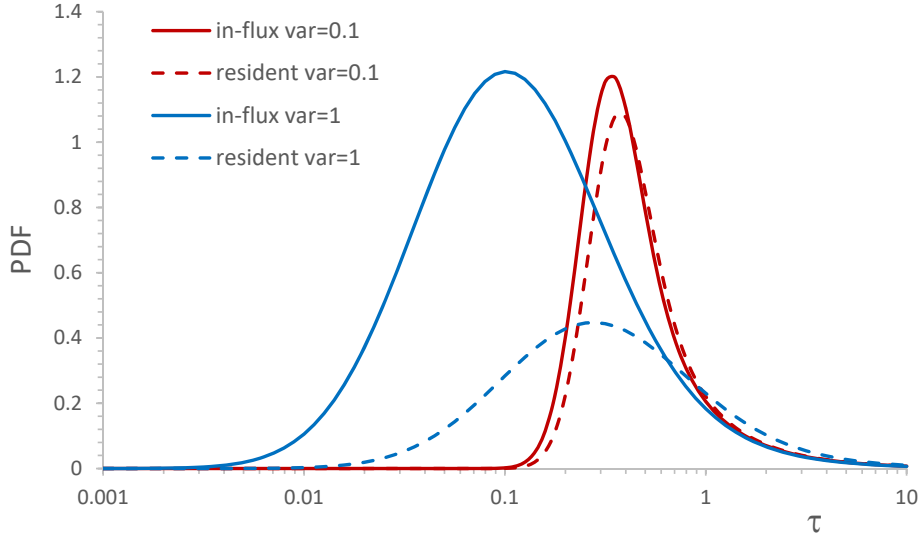


Figure 4: Comparison between the travel time PDFs pertaining to flux-proportional ("in-flux"; solid lines) and resident modes ("resident", dashed lines) injection conditions, for $\sigma_Y^2 = 0.1$ (red lines) and $\sigma_Y^2 = 1$ (blue lines).

243 Beetem, 1971; Koplik, 2001).

244 The spatial distribution of conductivity present in the aquifer system fur-
 245 ther enhances the above dispersion of solute, as visible in the curves of Fig-
 246 ures 2 and 3 for $\sigma_Y^2 > 0$. It is seen that, for increasing degree of heterogeneity
 247 σ_Y^2 , the travel time distributions depart from the solution for homogeneous
 248 formations in two ways: (i) a stronger preferential flow and (ii) a more per-
 249 sistent tail. Hence, the two main features of f_τ^F discussed before are further
 250 strengthened by the medium heterogeneity. The increase of preferential flow,
 251 and hence a faster rising limb of the PDF and a peak higher and closer to
 252 $\tau = 0$, is the results of the availability of highly conductive layers in the
 253 system, the relative numbers of which increases with heterogeneity σ_Y^2 .

254 The second feature observed in heterogeneous systems is also a stronger
 255 and more persistent tail as compared to the homogeneous case. Such behav-
 256 ior is determined by the combination of long and slow solute paths in the

257 low conductive layers that are present in heterogeneous systems; again, the
258 number of such low- K elements increases with σ_Y^2 . Altogether, the impact
259 of heterogeneity manifests in a significant spreading of solute particles that
260 increases the natural tendency to spreading induced by the dipole setup.

261 We emphasize that the injection mode, flux proportional or resident con-
262 centration, has a strong impact on the travel time distribution, especially
263 for highly heterogeneous formations. In Figure 4, we show the PDF of τ
264 for the two injection conditions above for a log-normally distributed K , i.e.
265 formula (11) and (8), respectively, for a low ($\sigma_Y^2 = 0.1$) and mild heteroge-
266 neous formation ($\sigma_Y^2 = 1$). Clearly, the effect of the injection condition is
267 small to negligible when heterogeneity is small, while it is important when
268 heterogeneity increases. In particular, the resident concentration injection
269 condition generally leads to a less pronounced preferential flow and a heavier
270 tail.

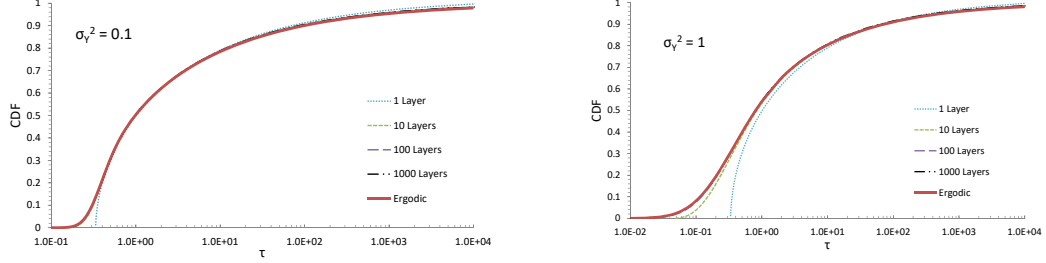
271 We note that similar results were observed by Pedretti and Fiori (2013)
272 for the convergent tracer test, in particular regarding the emergence of fast,
273 preferential flows when in presence of strongly heterogeneous formations.
274 Such feature mostly affects the early limb of the BTC. Instead, the BTC
275 tail is in the present case mostly affected by the particular flow configuration
276 determined by the dipole, which is very much different from the convergent
277 flow considered by Pedretti and Fiori (2013).

278 4. Impact of aquifer thickness (non-ergodicity)

279 As previously mentioned, the solutions derived in Section 2 are formally
280 valid for an ergodic system, i.e. when the number of layers is large enough
281 that the conductivity distribution f_K is adequately sampled over the aquifer
282 depth L ; such conditions require $L/I \gg 1$. Since the vertical integral scale
283 of conductivity I is usually of the order of $0.1m$ (Rubin, 2003, Table 2.1),
284 the latter condition may be met in applications.

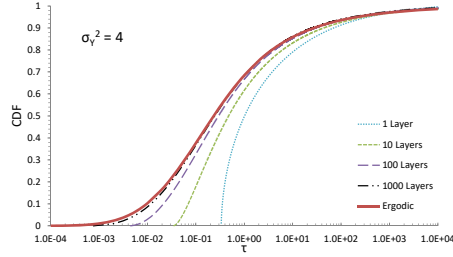
285 Still, it is worth exploring the travel time PDF under non-ergodic con-
286 ditions, i.e. for moderate or small L/I , and check the conditions for the
287 departure of the travel time PDF from the ergodic solutions derived in Sec-
288 tion 2. Once again we assume in the following f_τ^F for a log-normal K as
289 reference for the ergodic solution, i.e. formula (11).

290 The travel time PDF for a finite number of layers $N = L/(2I)$ can be
291 easily obtained by a simple Monte Carlo numerical procedure, along the fol-
292 lowing lines: (i) a vector of N random conductivities drawn from a given

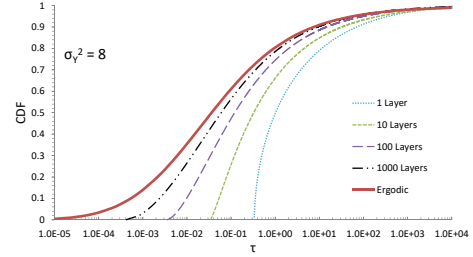


(a)

(b)



(c)



(d)

Figure 5: The mean travel time CDF for a few values of the number of layers N of the porous formation, for $\sigma_Y^2 = 0.1, 1, 4, 8$ (panels a,b,c,d).

293 CDF for K (f_K log-normal in the following examples) is generated, i.e.
 294 K_i ($i = 1, \dots, N$); (ii) for each K_i a set of travel times is calculated from
 295 equation (2) after discretization of θ in the interval $[0; \pi]$; (iii) the whole
 296 set of travel times for all layers are sorted and a cumulative frequency distribu-
 297 tion is obtained. The entire procedure (i)-(iii) is repeated N_{MC} times,
 298 generating N_{MC} cumulative frequency distributions that are averaged in order
 299 to obtain f_τ^F for a formation of given thickness $L = 2NI$. The procedure
 300 is very simple and can be easily coded. Although it can also provide the
 301 bands of uncertainty of f_τ^F , in the following we shall focus for brevity on f_τ^F
 302 only, i.e. the ensemble average.

303 The principal results of the above procedure are represented in Figure 5
 304 that display f_τ for four degrees of heterogeneity σ_Y^2 (four panels) and a few

305 values of N . The limiting cases are the case $N = 1$ corresponding to the
306 solution for a homogeneous formations, and the ergodic solution (formula
307 11) which is represented as a red thick line.

308 Starting from low heterogeneous formations ($\sigma_Y^2 = 0.1$, panel a), most of
309 the curves collapse to the ergodic solution when $N \approx 10$ and above. Hence,
310 a relatively small aquifer thickness is needed in order to reach ergodic con-
311 ditions in the test, and the ergodic solution can be safely applied in aquifers
312 of low heterogeneity. A similar situation happens for mild heterogeneity
313 ($\sigma_Y^2 = 1$, panel b), for which, however, the number of layers needed to reach
314 ergodic conditions are larger than the previous case. Such increase is more
315 consistent for highly heterogeneous systems ($\sigma_Y^2 = 4$, panel c), and more so
316 for $\sigma_Y^2 = 8$ (panel d), for which a relatively high number of layers ($N \geq 1000$)
317 needs to be sampled to get to ergodic conditions. The reasons for this behav-
318 ior is simple: when the variance σ_Y^2 grows, the log-conductivity distribution
319 becomes broad and a larger sample size is needed in order to capture it. We
320 note again that a similar result was observed by Pedretti and Fiori (2013) for
321 the convergent tracer test, although such sampling problems always occurs
322 when dealing with highly heterogeneous random fields.

323 Thus, under non-ergodic conditions the ergodic solutions developed in this
324 work may overestimate the BTC spreading when applied to a tracer test. In
325 particular, if such solutions are employed for the aquifer characterization, as
326 discussed in the next Section, the inferred σ_Y^2 may be underestimated when
327 in presence of highly heterogeneous aquifers.

328 5. Conductivity characterization by the dipole test with applica- 329 tion examples

330 The solution developed in this work can be used for the characterization
331 of hydraulic conductivity K . In particular, the results of a dipole test can
332 be interpreted through the analytical solution for f_τ developed in Section 2
333 to determine the log-conductivity variance σ_Y^2 , which epitomizes the degree
334 of heterogeneity in the aquifer. For instance, assuming a log-normal K , ex-
335 pressions (14,15) can be fitted to the experimental BTC in order to obtain
336 σ_Y^2 . We emphasize, however, that the solutions (10,12) are for a generic dis-
337 tribution f_K , and in principle even a numerical one could be employed. The
338 elements of f_τ that are mostly impacted by the conductivity heterogeneity is
339 the first segment, i.e. the rising limb and the peak, and the fitting procedure
340 is typically influenced by that part. Instead, the effects of σ_Y^2 on the tail are

341 less relevant because the tail is anyway influenced by the later arrivals of the
342 particles characterized by the longest (and slowest) path lines.

343 In the following we show a few application examples. In all cases a log-
344 normal f_K is assumed, and hence the solution (11) is employed for the fitting
345 of the experimental data. The fitting of tracer tests depends on several
346 different factors, like e.g. the choice of the objective function, the weight
347 given to data points, the part of the BTC of interest, to mention some;
348 thus, the fitting method typically depends on the experience and preference
349 of the modeler. For the sole purpose of illustration we have adopted here
350 a simple least-square fit method, with an a-posteriori visual check that the
351 fitted curves have a reasonable behavior.

352 The parameters employed in the applications, as well as the fitted log-
353 conductivity variance, are reproduced in Table 1. The results are represented
354 in terms of either concentration C , relative concentration C/C_0 or the CDF
355 of travel time, depending on the presentation of the results in the source
356 papers.

357 In order to support the novelty of our approach, the equivalent homo-
358 geneous solution for advective-dispersive flow to a pumping well in a dipole
359 test was calculated for all three examples. Therefore, the model by Hoopes
360 and Harleman (1967) (their Eq. 26), similar to the one developed by Gelhar
361 (1982), was implemented here. The model accounts for mixing along stream-
362 lines but neglects mixing between streamlines and adopts a few analytical
363 approximations, such that the solution is limited to small values of α/a , with
364 α the equivalent longitudinal dispersivity. We anticipate that the homoge-
365 neous model can reasonably capture the experimental data only for small
366 heterogeneity of the porous medium, but fails for heterogeneous formations.
367 Furthermore, the fitted dispersivities α are relatively large compared to the
368 well distance a , beyond the range of validity of the solution, as also visible
369 by the non-zero concentration for $t = 0$. This shows that the application
370 of the equivalent homogeneous solution can be problematic for mild/high
371 heterogeneity since it is formally only valid for small dispersivities α .

372 5.1. MADE

373 A dipole tracer experiment (referred to as MADE-5) was performed in
374 2008 at the Columbus Air Force Base in Columbus, Mississippi, commonly
375 known as the MADE (MAcro Dispersion Experiment) site. The main aim
376 of the test was to investigate the influence of small-scale mass-transfer and
377 dispersion processes on well-to-well transport. Test settings and results are

Table 1: Parameters of the study cases.

Symbol	Parameter	MADE	Mobile	Barstow
Q	discharge [m ³ /h]	0.34	56.76	12.5
n	porosity [-]	0.32	0.35	0.30
$2a$	distance between wells [m]	6.0	38.3	6.4
L	aquifer thickness [m]	8.1	21.6	27.5
C_0	initial concentration [mg/L]	1000	169	-
Δ	duration of pulse [h]	6	76.6	84
σ_Y^2	estimated log-conductivity variance [-]	4.1	0.24	0.5

378 presented in detail in line with a numerical model of the experiment by
 379 Bianchi et al. (2011). Details on aquifer characteristics and parameters of
 380 the dipole test are summarized in Table 1.

381 Four wells have been installed for the dipole test. The injection and
 382 extraction well are located 6 m apart and two multi-level sampling wells were
 383 installed in between, at distances of 1.5 m and 3.75 m from the injection well.
 384 The BTCs were measured at the extraction well as well as at seven different
 385 depths in the two multi-level sampling wells.

386 The test was performed in 3 phases: Initially clean water was injected
 387 for 48 h at a rate of 5.68 l/min. After a relative steady state flow field was
 388 established, 2078 l of bromide solution with a concentration of 1000 mg/l was
 389 introduced into the aquifer within 366 min. Clean water was injected again
 390 during the third phase until the experiment was finished after 32 days from
 391 injection.

392 Multiple hydrogeological, geophysical investigations as well as tracer tests
 393 have been performed since the MADE site was established with the motiva-
 394 tion to gain new insights into transport in highly heterogeneous aquifers (for
 395 details see e.g. Zheng et al. (2011)). Thus, for this site detailed geostatistical
 396 information is available for comparison. The following values for geometric
 397 mean of hydraulic conductivity and variance of log-conductivity as the one-
 398 point statistical parameters were reported: Interpretation of the flowmeter
 399 measurements resulted in $K_G = 4.3 \cdot 10^{-5}$ m/s and $\sigma_Y^2 = 4.4 \pm 1$ whereas the
 400 DPIL observations deliver values of $K_G = 6.7 \cdot 10^{-6}$ m/s and $\sigma_Y^2 = 5.9 \pm 1.5$
 401 (Bohling et al., 2012, 2016).

402 A fit of the analytical curve provided in this work with the experimental
 403 data is given in Figure 6, and the estimated log-conductivity variance is
 404 about $\sigma_Y^2 = 4$. Such value is lower than the recent DPIL-based estimate by

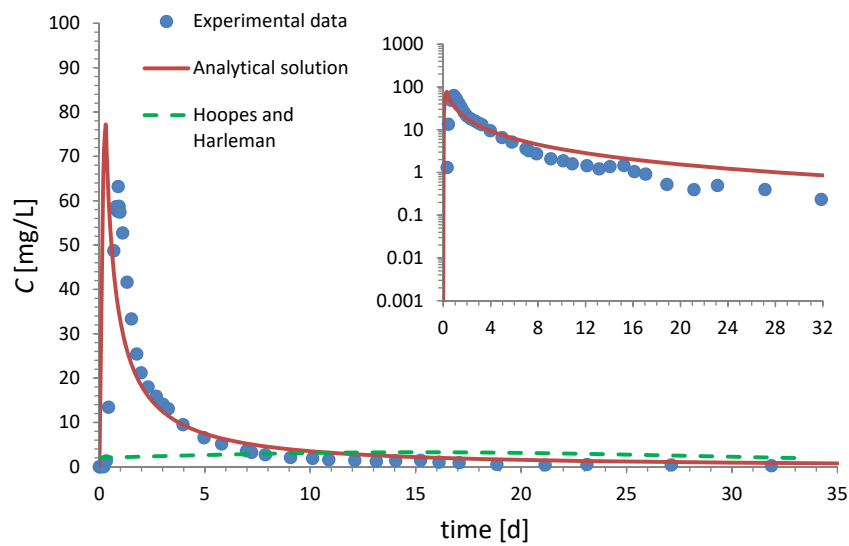


Figure 6: Experimental results of the dipole tracer test at the MADE site and its interpretation by the proposed analytical model as well as the equivalent homogeneous solution of Hoopes and Harleman (1967); experimental data from Bianchi et al. (2011).

405 Bohling et al. (2016), that is $\sigma_Y^2 = 5.9$ with a 95% confidence interval of
406 [4.4; 7.4], being close to the lower bound; instead, the inferred value is closer
407 to the one obtained by flowmeter measurements. The differences between the
408 two estimates might be explained by either the different areas of the MADE
409 site explored by the two methods, where the DPIL analysis covered a much
410 larger domain than the one related to the dipole test, or, more likely, by
411 non-ergodic effects, as discussed at the end of Section 4.

412 The good fit of the analytical solution to the experimental data not only
413 for the peak (although with some temporal anticipation), but also for the
414 tailing behavior can be nicely seen in the insert semi-log plot in Figure 6.
415 A direct comparison to Figure 7 of Bianchi et al. (2011) shows that the
416 analytical curve based on an ADE approach can reproduce the concentration
417 distribution similarly good as the dual domain model fitted by Bianchi et al.
418 (2011).

419 It can be seen that an equivalent homogeneous transport model (solution
420 of Hoopes and Harleman (1967), with optimal fit of dispersivity $\alpha = 2.73$ m)
421 can neither reproduce the heavy peak behavior nor the tailing which is ob-
422 viously strongly impacted by the strong aquifer heterogeneity.

423 5.2. Mobile

424 Molz et al. (1986) and Huyakorn et al. (1986b) presented and analyzed
425 the results of a two well tracer test with pulse input of bromide at a site near
426 Mobile, Alabama. The sites formation is composed of a low-terrace deposit
427 of Quaternary age consisting of interbedded sands and clays which have been
428 deposited along the western edge of the Mobile River. The sandy confined
429 aquifer section is about 20 m thick and located between 40 m and 60 depth.

430 The two-well tracer test was performed making use of two fully pene-
431 trating wells in a distance of 38.3 m. Equal injection and withdrawal rate
432 average to 0.946 m³/min. A slug of bromide as tracer was added to the in-
433 jection water during the first 76.6 hours of the experiment which persisted in
434 total 32.5 days. Since the withdrawn water was re-injected the tracer recir-
435 culated. Details on aquifer characteristics and parameters of the dipole test
436 are summarized in Table 1.

437 Investigation of hydraulic conductivity distribution have been performed
438 by Molz et al. (1990) based on impeller meter measurements and small scale
439 pumping tests. Results lead to the conclusion that the study aquifer is fairly
440 homogeneous. They reported a mean value of hydraulic conductivity of

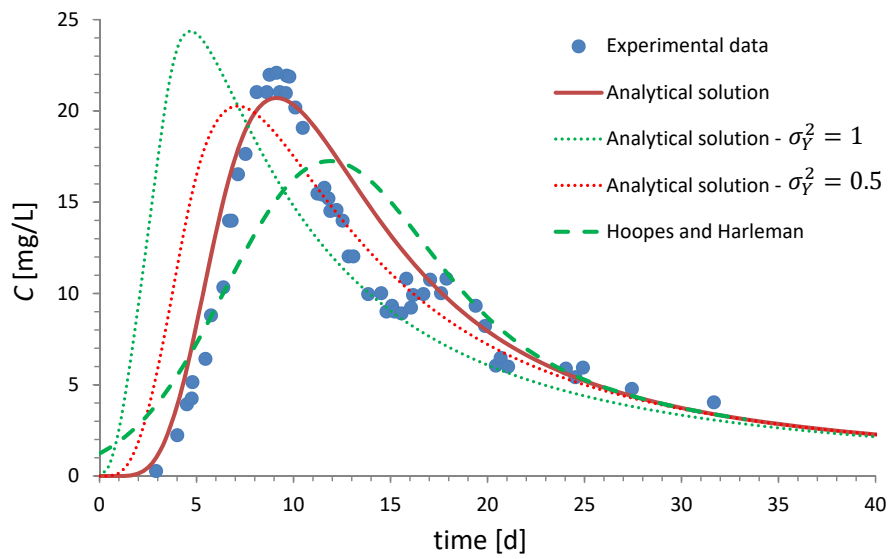


Figure 7: Experimental results of the dipole tracer test at the Mobile site and its interpretation by the proposed analytical model as well as the equivalent homogeneous solution of Hoopes and Harleman (1967); experimental data from Molz et al. (1986).

441 54.9 m/day with a standard deviation of only 2.4 m/day. Further geosta-
442 tistical analysis for the hydraulic conductivity at that site are not known to
443 the authors.

444 Figure 7 shows a fit of the analytical curve provided in this work with
445 the experimental data. The very small value of $\sigma_Y^2 = 0.24$ inferred for the
446 estimated log-conductivity variance supports the findings that the Mobile
447 aquifer is weakly heterogeneous. In addition, Figure 7 gives a simple sensi-
448 tivity analysis with the analytical curve for two higher variances of $\sigma_Y^2 = 0.5$
449 and $\sigma_Y^2 = 1$ showing that the solution is typically quite sensitive towards
450 the log-conductivity variance but mostly for the early-time behavior and the
451 peak. The tail is mostly dominated by the arrival times of the different flow
452 paths giving a diminishing impact of the heterogeneity on late time BTC
453 behavior. Furthermore, the best fit of the equivalent homogeneous solution
454 of Hoopes and Harleman (1967) (dispersivity $\alpha = 4.06$ m) to the data indi-
455 cates that although the aquifer is mildly heterogeneous a purely homogeneous
456 solution is not able to adequately reproduce the concentration distribution.

457 5.3. Barstow

458 Robson (1974) reported the results of a small scale dipole tracer test in
459 the Barstow's aquifer which consist of very permeable younger alluvium of
460 Holocene age deposited by the Mojave River and alluvial fans. The injection
461 and withdrawal wells are located in a distance of 6.4 m, both were perforated
462 through most of the 27.45 m aquifer thickness. A recharge/discharged rate
463 of 55 gallons per minute was reported. The tracer solution of sodium chlo-
464 ride was constantly injected during the 84-hour span of the test. Since the
465 withdrawn water was re-injected the tracer recirculated.

466 Concentration was measured at temporal intervals of more than 4 h, giv-
467 ing a sparse database in particular for the early time of the BTC. The test was
468 originally analyzed making use of the method of Grove and Beetem (1971) to
469 estimate values of macrodispersivity. As pointed out by Robson (1974), the
470 late time behavior of the concentration curve should be taken with caution
471 due to the tracer recirculation that was carried out during the test. Details
472 on aquifer characteristics and parameters of the dipole test are summarized
473 in Table 1. Geostatistical analysis for the hydraulic conductivity at that site
474 are not known to the authors.

475 A fit of the analytical curve with the experimental data is given in Figure 8
476 with an estimated log-conductivity variance of $\sigma_Y^2 = 0.5$. along with the
477 best fit for the equivalent homogeneous solution of Hoopes and Harleman

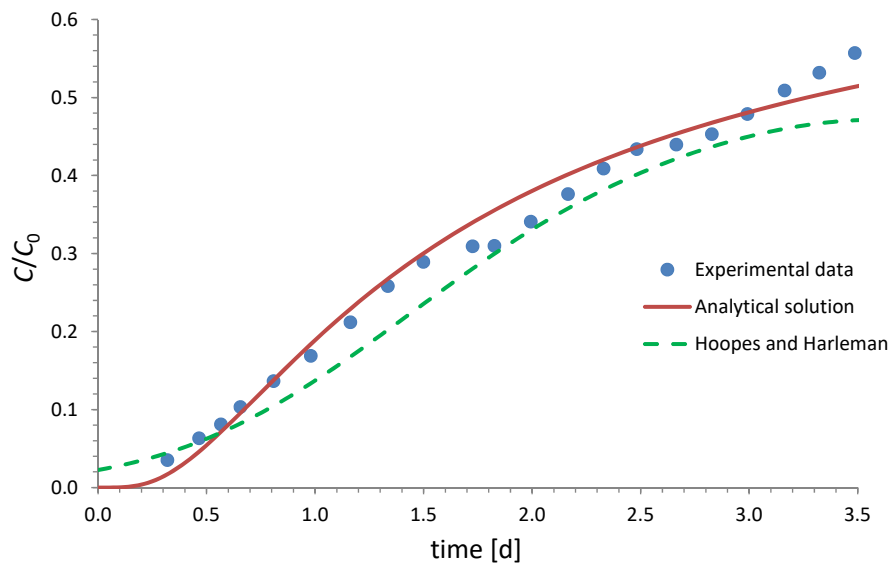


Figure 8: Experimental results of the dipole tracer test at the Barstow site and its interpretation by the proposed analytical model as well as the equivalent homogeneous solution of Hoopes and Harleman (1967); experimental data from Robson (1974).

478 (1967) (fitted dispersivity of $\alpha = 0.98$). Since no geostatistical analysis of
479 the hydraulic conductivity in the aquifer is known, there is no reference for
480 comparison. However, the fit of the analytical curves with the measured
481 data shows nicely how the shape of the BTC can be related to the aquifer
482 heterogeneity by the log-conductivity variance rather than dispersivity.

483 6. Summary and Conclusions

484 In this paper, we derived a new analytical solution for interpreting dipole
485 tests in heterogeneous media. Furthermore, it was presented how the solu-
486 tion can be used for interpretation of dipole field test in view of geostatistical
487 aquifer characterization. The work was motivated by the lack of methods for
488 dipole tests taking the strong spatial heterogeneity of hydraulic conductivity
489 into account, although tracer tests are central tools for inferring hydrogeo-
490 logical, structural and transport parameters of the subsurface.

491 In dipole tracer tests, also two-well test or doublet tests, a tracer is intro-
492 duced at a recharge well and the breakthrough curve (BTC) is measured at a
493 pumping well. The analytical solution for the BTC at the pumping well was
494 developed by considering a stratified heterogeneous hydraulic conductivity
495 structure. The analysis of the BTC in this kind of media was carried out by
496 considering the travel time of a generic solute particle, from the injection to
497 the pumping well. The derivation of the analytical solutions was performed
498 for two different injection conditions: (i) resident concentration, assuming
499 that the mass of solute entering each layer from the injection well is constant
500 for all layers; and (ii) flux proportional injection mode where the entering
501 mass is assumed proportional to layer conductivity. The solution was derived
502 for an instantaneous pulse of solute and extended to a formula for continuous
503 solute injections.

504 The illustration of results focused on different aspects of the solution: (i)
505 the impact of heterogeneity; (ii) the impact of the injection condition; and
506 (iii) the impact of non-ergodic conditions at the injection well. The analysis
507 lead to the following conclusions:

- 508 • The impact of heterogeneity manifests in a significant spreading of so-
509 lute particles that increases the natural tendency to spreading induced
510 by the dipole setup. For a log-normal conductivity distribution an in-
511 creasing degree of heterogeneity leads to a stronger preferential flow
512 and a more persistent tail.

- 513 • The injection mode has a strong impact on the travel time distribution,
514 especially for highly heterogeneous formations. The resident concentra-
515 tion injection condition generally leads to a less pronounced preferential
516 flow and a heavier tail.
- 517 • With increasing heterogeneity the number of layers needed to reach
518 ergodic conditions become larger. Under non-ergodic conditions the
519 solutions developed in this work may overestimate the BTC spreading.
520 In particular, if such solutions are employed for the aquifer characteriza-
521 tion, the inferred log-conductivity variance σ_Y^2 may be underestimated
522 when in presence of highly heterogeneous aquifers.

523 In final step, the derived method was used for conductivity characteri-
524 zation at three dipole field tests as illustrative examples. Thereby, the log-
525 conductivity variance was inferred from the shape of the observed BTCs.
526 The analysis of dipole tests at two sites indicated a mild heterogeneity, being
527 in line with other observations at these sites. The dipole test performed at
528 the heterogeneous MADE site was analyzed resulting in a high value of vari-
529 ance being in the same range as an geostatistical interpretation of flowmeter
530 measurements but smaller than the variance resulting from a geostatistical
531 interpretation of DPIL measurements. This result can be associated to the
532 assumption of ergodicity in the analytical solution which might not be present
533 at the heterogeneous field site giving an underestimation of variance by the
534 analytical solution.

535 The presented method is the first fully analytical tool for dipole tracer
536 test analysis taking heterogeneity of hydraulic conductivity into account.
537 Assumptions in the derivation of the analytical solutions have been taken to
538 be in line with the conditions encountered in the field. It could be shown
539 that the method is easily applicable to measured BTCs for inferring the
540 degree of heterogeneity, namely the log-conductivity variance. The method is
541 a promising geostatistical analyzing tool as addition to other geostatistical
542 investigations methods, often being time- and cost-intensive.

543 Acknowledgements

544 We are grateful to Marco Bianchi for providing the data of the MADE-5
545 experiments. Furthermore, we would like to thank Fred Molz for provid-
546 ing background information of the Mobile test site and Sebastian Mller for
547 support with computations.

548 **References**

- 549 Bianchi, M., Zheng, C., Tick, G. R., Gorelick, S. M., 2011. Investigation of
550 Small-Scale Preferential Flow with a Forced-Gradient Tracer Test. *Ground*
551 *Water* 49 (4), 503–514.
- 552 Bohling, G. C., Liu, G., Dietrich, P., Butler, J. J., 2016. Reassessing the
553 MADE direct-push hydraulic conductivity data using a revised calibration
554 procedure. *Water Resour. Res.* 52 (11), 8970–8985.
- 555 Bohling, G. C., Liu, G., Knobbe, S. J., Reboulet, E. C., Hyndman, D. W.,
556 Dietrich, P., Butler, J. J., 2012. Geostatistical analysis of centimeter-scale
557 hydraulic conductivity variations at the MADE site. *Water Resour. Res.*
558 48, W02525.
- 559 Claassen, H., Cordes, E., 1975. Two-Well Recirculating Tracer Test in Frac-
560 tured Carbonate Rock, Nevada. *Hydrological Sciences Bulletin* 20 (3), 367–
561 382.
- 562 Dagan, G., 1990. Transport in heterogeneous porous formations: Spatial
563 moments, ergodicity, and effective dispersion. *Water Resour. Res.* 26 (6),
564 1281–1290.
- 565 Gelhar, L., 1993. *Stochastic Subsurface Hydrology*. Prentice Hall, Englewood
566 Cliffs, N. Y.
- 567 Gelhar, L. W., 1982. Analysis of two-well tracer tests with a pulse input.
568 Tech. Rep. RHO-BW-CR-131 P, Rockwell Int., Richland, Wash.
- 569 Gelhar, L. W., Collins, M. A., 1971. General analysis of longitudinal disper-
570 sion in nonuniform flow. *Water Resour. Res.* 7 (6), 1511–1521.
- 571 Grove, D. B., Beetem, W. A., 1971. Porosity and dispersion constant calcu-
572 lations for a fractured carbonate aquifer using the two well tracer method.
573 *Water Resour. Res.* 7 (1), 128–134.
- 574 Hoopes, J. A., Harleman, D. R. F., 1967. Waste water recharge and dispersion
575 in porous media. *Journal of the Hydraulics Division* 93 (5), 51–71.
- 576 Huyakorn, P. S., Andersen, P. F., Güven, O., Molz, F. J., 1986a. A curvilinear
577 finite element model for simulating two-well tracer tests and transport in
578 stratified aquifers. *Water Resour. Res.* 22 (5), 663–678.

- 579 Huyakorn, P. S., Andersen, P. F., Molz, F. J., Güven, O., Melville, J. G.,
580 1986b. Simulations of two-well tracer tests in stratified aquifers at the
581 Chalk River and the Mobile Sites. *Water Resour. Res.* 22 (7), 1016–1030.
- 582 Hyndman, D. W., Gorelick, S. M., 1996. Estimating lithologic and trans-
583 port properties in three dimensions using seismic and tracer data: The
584 Kesterson aquifer. *Water Resour. Res.* 32 (9), 2659–2670.
- 585 Jankovic, I., Fiori, A., 2010. Analysis of the impact of injection mode in
586 transport through strongly heterogeneous aquifers. *Adv. Water Resour.*
587 33 (10), 1199–1205.
- 588 Koplik, J., 2001. The tracer transit-time tail in multipole reservoir flows.
589 *Transp. Porous Media* 42 (1-2), 199–209.
- 590 Matheron, G., De Marsily, G., 1980. Is transport in porous media always
591 diffusive? a counterexample. *Water Resour. Res.* 16 (5), 901–917.
- 592 Mercado, A., 1967. The spreading pattern of injected water in a permeability
593 stratified aquifer. IAHS Press, pp. 23–36.
- 594 Molz, F. J., Güven, O., Melville, J. G., Crocker, R. D., Matteson, K. T.,
595 1986. Performance, analysis, and simulation of a two-well tracer test at
596 the Mobile Site. *Water Resour. Res.* 22 (7), 1031–1037.
- 597 Molz, F. J., Gven, O., Melville, J. G., Cardone, C., 1990. Hydraulic Con-
598 ductivity Measurements at Different Scales and Contaminant Transport
599 Modelling. In: *Dynamics of Fluids in Hierarchical Porous Media*. Aca-
600 demic Press, London.
- 601 Papoulis, A., 1991. *Probability, Random Variables, and Stochastic Processes*.
602 McGraw-Hill.
- 603 Pedretti, D., Fiori, A., 2013. Travel time distributions under convergent ra-
604 dial flow in heterogeneous formations: Insight from the analytical solution
605 of a stratified model. *Advances in Water Resources* 60, 100–109.
- 606 Pickens, J. F., Grisak, G. E., 1981. Scale-dependent dispersion in a stratified
607 granular aquifer. *Water Resour. Res.* 17 (4), 1191–1211.

- 608 Robson, S. G., 1974. Feasibility of digital water-quality modeling illustrated
609 by application at Barstow, California. Tech. Rep. WRI - 73-46, U. S. Geol.
610 Surv.
- 611 Rubin, Y., 2003. Applied Stochastic Hydrogeology. Oxford Univ. Press, New
612 York.
- 613 Thorbjarnarson, K. W., Mackay, D. M., 1997. A field test of tracer trans-
614 port and organic contaminant elution in a stratified aquifer at the Rocky
615 Mountain Arsenal (Denver, Colorado, U.S.A.). *J. Contam. Hydrol.* 24 (3-
616 4), 287-312.
- 617 Webster, D. S., Proctor, J. F., Marine, I. W., 1970. Two-well tracer test in
618 fractured crystalline rock. Tech. Rep. WSP - 1544-I, United States Geo-
619 logical Survey.
- 620 Welty, C., Gelhar, L. W., 1989. Evaluation of longitudinal dispersivity from
621 tracer test data. Tech. Rep. 320, M.I.T. Press, Cambridge, Mass.
- 622 Wilson, L. G., 1971. Investigations on the subsurface disposal of waste ef-
623 fluents at inland sites. Res. Dev. Prog. Rep. 650, U.S. Dep. of the Inter.,
624 Washington, D.C.
- 625 Zheng, C., Bianchi, M., Gorelick, S. M., 2011. Lessons learned from 25 years
626 of research at the MADE site. *Ground Water* 49 (5), 649-662.